⑫ **LEVEL** II

⑭ AFGL-TR-79-0254 PAPERS, NO. 690

AFGL-ERP-689

ADA086861

⑥

Comparison of Results From the S3-2 Satellite and the Chatanika Radar in an Early Morning Aurora

⑩ ROGER P. VANCOUR
BERTRAM M. SHUMAN

④ *Environmental research papers*

⑫ 18

⑪ 22 Oct 79

⑯ PROJECT 2311   ⑰ G-1

SPACE PHYSICS DIVISION
AIR FORCE GEOPHYSICS LABORATORY
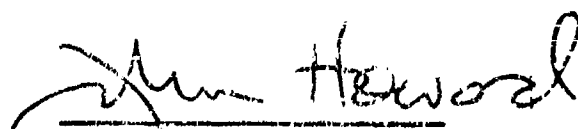HANSCOM AFB, MASSACHUSETTS 01731

AIR FORCE SYSTEMS COMMAND, USAF

409575   80 7 16 004

This report has been reviewed by the ESD Information Office (OI) and is releasable to the National Technical Information Service (NTIS).

This technical report has been reviewed and is approved for publication.

FOR THE COMMANDER

Chief Scientist

REPORT DOCUMENTATION PAGE	READ INSTRUCTIONS BEFORE COMPLETING FORM

1. REPORT NUMBER	2. GOVT ACCESSION NO.	3. RECIPIENT'S CATALOG NUMBER
AFGL-TR-79-0254	AD-A086861	

4. TITLE (and Subtitle)	5. TYPE OF REPORT & PERIOD COVERED
COMPARISON OF RESULTS FROM THE S3-2 SATELLITE AND THE CHATANIKA RADAR IN AN EARLY MORNING AURORA	Scientific. Interim.
	6. PERFORMING ORG. REPORT NUMBER
	ERP No. 680

7. AUTHOR(s)	8. CONTRACT OR GRANT NUMBER(s)
Roger P. Vancour Bertram M. Shuman	

9. PERFORMING ORGANIZATION NAME AND ADDRESS	10. PROGRAM ELEMENT, PROJECT, TASK AREA & WORK UNIT NUMBERS
Air Force Geophysics Laboratory (PH) Hanscom AFB Bedford, MA 01731	61102F 2311G105

11. CONTROLLING OFFICE NAME AND ADDRESS	12. REPORT DATE
Air Force Geophysics Laboratory (PH) Hanscom AFB Bedford, MA 01731	22 October 1979
	13. NUMBER OF PAGES
	17

14. MONITORING AGENCY NAME & ADDRESS(if different from Controlling Office)	15. SECURITY CLASS. (of this report)
	Unclassified
	15a. DECLASSIFICATION DOWNGRADING SCHEDULE

16. DISTRIBUTION STATEMENT (of this Report)

Approved for public release; distribution unlimited.

17. DISTRIBUTION STATEMENT (of the abstract entered in Block 20, if different from Report)

18. SUPPLEMENTARY NOTES

19. KEY WORDS (Continue on reverse side if necessary and identify by block number)
S3-2 satellite
Chatanika radar
Aurora
Magnetic fields
Electron electrostatic analyzer

20. ABSTRACT (Continue on reverse side if necessary and identify by block number)
During orbit 6352, the Air Force satellite S3-2 passed by the Chatanika radar in a trajectory that was only 12° off from the geomagnetic meridian along which the radar scanned. This report presents the analysis of the data for this orbit from the triaxial fluxgate magnetometer, the electrostatic analyzer aboard the satellite, and the radar data. These data were obtained simultaneously during a morning active aurora. Comparisons of current densities determined by these experiments are made, and the agreement between

DD FORM 1473 EDITION OF 1 NOV 65 IS OBSOLETE

the electrostatic analyzer precipitating electron fluxes and the electron densi-
ties determined from the radar data is shown.

Contents

Illustrations

Tables

Comparison of Results From the S3-2 Satellite and the Chatanika Radar in an Early Morning Aurora

1. INTRODUCTION

Orbit 6352 of the S3-2 satellite provides a singularly favorable instance of a close by-pass with the Chatanika ground-based radar during an active morning aurora. Figure 16[1] shows that the satellite passed within 60 km of Chatanika with its orbital track only 12° off from the geomagnetic meridian direction, along which the Chatanika radar makes its altitude-scan observations. Data from both sources were taken simultaneously, allowing for a direct comparison between the radar-inferred ionospheric parameters and those derived from in-situ measurements of the satellite. This paper discusses the results of the triaxial fluxgate magnetometer and the electrostatic analyzer (ESA) on the satellite and the Chatanika radar for this orbit.

1. Vondrak, R. R. (1979) Simultaneous Measurements of the Auroral Ionosphere by the Chatanika Radar and the S3-2 Satellite, AFGL-TR-79-0048.

2. SCIENTIFIC EXPERIMENTS

2.1 Chatanika Radar

The Chatanika radar was operated in an elevation-scan mode for several hours prior to the S3-2 pass. The latitudinal extent of the 100 km altitude measurements during these scans is shown in Figure 16.[1] They are along the geomagnetic meridian direction extending from about 300 km north to 200 km south of Chatanika. The satellite came into the auroral oval at about 15:07 UT and passed through the region of interest between 15:09 and 15:10:30 UT.

2.2 Triaxial Fluxgate Magnetometer

A triaxial fluxgate magnetometer, with the sensor extended 20 feet from the body of the spacecraft, provided high-resolution component measurements of the geomagnetic field. A model earth's field, IGRF 1975, suitably updated, was subtracted leaving residuals near zero gammas. ΔB_y, the residual of the y-component in the spacecraft's principal axis system, was in the nominal east-west direction and is shown plotted in Figure 1. The sinusoid superimposed on the plot is due to

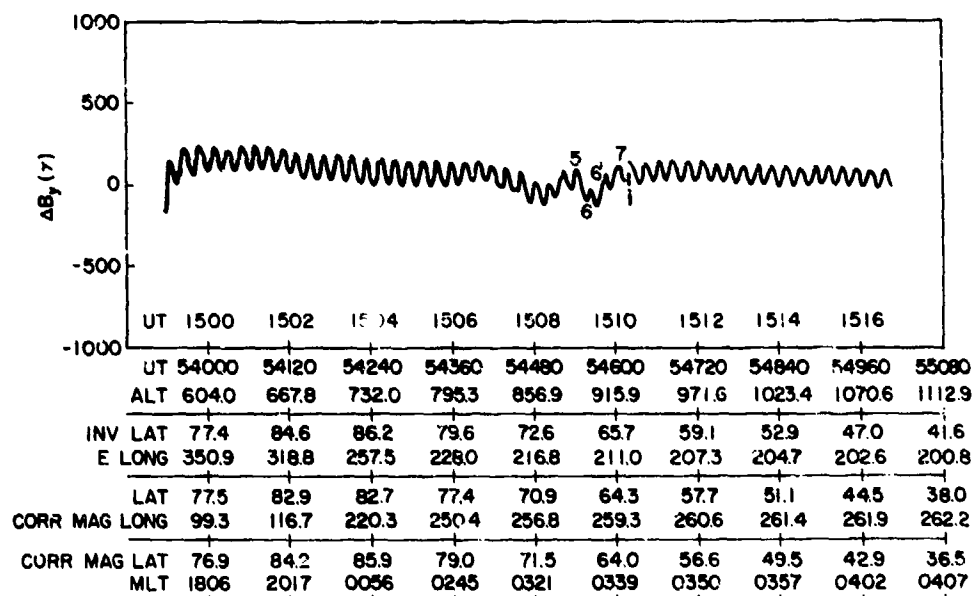|	UT	1500	1502	1504	1506	1508	1510	1512	1514	1516
	UT	54000	54120	54240	54360	54480	54600	54720	54840	54960	55080
	ALT	604.0	667.8	732.0	795.3	856.9	915.9	971.6	1023.4	1070.6	1112.9
INV LAT		77.4	84.6	86.2	79.6	72.6	65.7	59.1	52.9	47.0	41.6
E LONG		350.9	318.8	257.5	228.0	216.8	211.0	207.3	204.7	202.6	200.8
LAT		77.5	82.9	82.7	77.4	70.9	64.3	57.7	51.1	44.5	38.0
CORR MAG LONG		99.3	116.7	220.3	250.4	256.8	259.3	260.6	261.4	261.9	262.2
CORR MAG LAT		76.9	84.2	85.9	79.0	71.5	64.0	56.6	49.5	42.9	36.5
MLT		1806	2017	0056	0245	0321	0339	0350	0357	0402	0407

Figure 1. Variation of the Nominal East-West Component, ΔB_y of the Magnetometer

6

the remnant spin modulation of the satellite. In the time interval 1507 to 1510, the magnetic signature of two pairs of up-and-down current sheets shows clearly when the satellite traversed the auroral oval. The southernmost portion, from 15:09 on, a downward and upward current, corresponds to the region that was close by the Chatanika radar field of view.

2.3 Electrostatic Analyzer (ESA)

The electrostatic analyzer collects electrons in the energy range oi 80 eV to 17 keV to produce a 32-point spectrum. The instrument is mounted so that its aperture is in the spin plane of the satellite. A more complete description of the magnetometer experiment may be found in Burke, et al.[2] and a description of the ESA is given by Morel et al.[3]

3. RESULTS OF MEASUREMENTS IN AN ACTIVE MORNING AURORA

The Chatanika radar data[1] has two curves, Figure 19*, showing the differential energy distribution of electrons when the radar was observing a point 27 km north of the radar, and a second point 55 km south of the radar, both at an altitude of 100 km and along the geomagnetic meridian direction. The electrostatic analyzer, in its spin cycle, passed through the range of pitch angles corresponding to precipitating electrons at 900 km altitude from 15:10:01.6 to 15:10:07.9 UT. The satellite passed through the field line connecting to the radar observation point at 100 km altitude, 27 km north of the radar near the end of this precipitating collection segment. Figure 2 shows a comparison of the radar data from Figure 19[1] corrected to the units of $(cm^2 sec sr keV)^{-1}$ and the differential energy spectrum of the electrostatic analyzer data averaged over the precipitation segment of the spin cycle. The radar data were taken about 3.5 minutes before the satellite data. Since the diffuse auroral form was quite stable, the two sets of data are compared, and are in good agreement between 2 to 10 keV, with similar spectral shapes.

---

*Data from Figure 19 (Vondrak, 1979) corrected and reproduced here as Figure 2.

2. Burke, W. J., Hardy, D. A., Rich, F. J., Kelley, M. C., Smiddy, M., Shuman, B., Sagalyn, R. C., Vancour, R. P., Wildman, P. J. L., Lai, S. T., and Bass, J. (1979) A Case Study of S3-2 Observations in the Late Evening Auroral Oval, AFGL-TR-79-0011.

3. Morel, P. R., Hanser, F. A., and Sellers, B. (1974) Design, Fabrication and Integration of an Electrostatic Analyzer for a Satellite Payload, AFCRL-TR-75-0017.
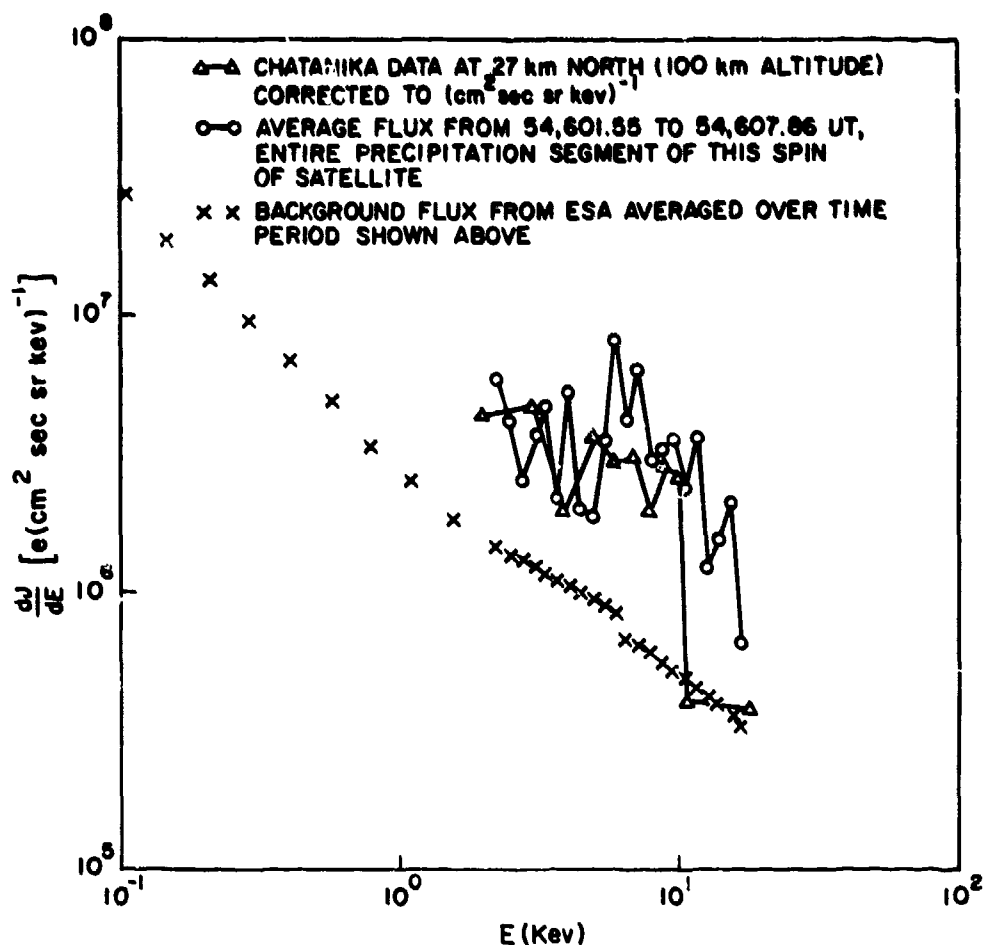
Figure 2. ESA Differential Flux Spectrum Averaged Over the Precipitation Period Near the Field Line of the Radar Observation Point (27 km North) and the Differential Spectrum Inferred From the Radar Data

The ESA passed through the next precipitation segment on the next spin cycle from 15:10:21.9 to 15:10:28.4 UT. The satellite passed through the field line connecting to the radar observation point at 100 km altitude, 55 km south of the radar, about 0.8 sec after starting this precipitation segment. However, between 15:10:21.9 and 15:10:25.2 UT, a 2-sec dropout occurred in the ESA data. During the remainder of this time period there were no counts recorded in any energy channels. From 15:10:25.2 (satellite is ≈ 20 km south of field line to radar observation point) to 15:10:28.4 UT, data were recorded in the pitch angle range range of 0.1° to 56.7°. The comparison of this data to the Chatanika data

9

is shown in Figure 3. The ESA data were averaged over this latter time period.
Since the Chatanika flux values, in some instances, are lower than the background
of ESA, the curves do not agree as well as in the first case but, nevertheless, are
within a factor of 2 with each other.

Using the model of field-aligned currents flowing up and down in parallel
infinite sheets oriented in the east-west direction, the current density may be
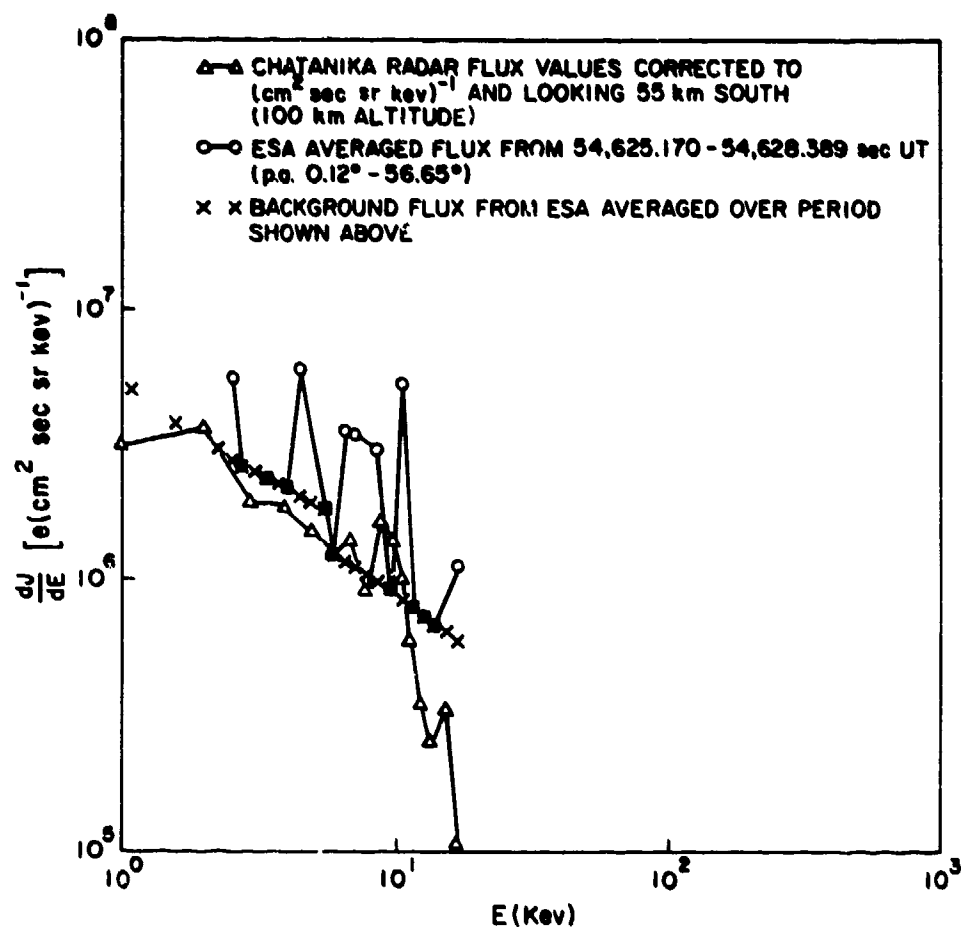calculated from the observed change in the east-west magnetic field component,

Figure 3. ESA Differential Flux Spectrum Averaged Over the Precipitation
Period Near the Field Line of Radar Observation Point (55 km South) and the
Differential Flux Inferred From the Radar Data

as the satellite traverses the current sheet in the north-south direction, as shown by

$$\frac{4\pi}{10} \; j_z (A/km^2) \approx \frac{\Delta B_y(v)}{\Delta x(km)} \; . \tag{1}$$

The quantity, $\frac{\Delta B_y}{\Delta x}$, the north-south gradient of the east-west magnetic field residual, was calculated from Figure 4 (provided by F. Rich). The scale has been expanded, the plot inverted, and the sinusoidal modulation removed. The field aligned current densities were determined from 54,543 (point 5, Figure 4) to 54,568 sec UT (point 6) to be $0.7\mu A/m^2$ downward, reversing to $0.6\mu A/m^2$ upward from 54,568 (point 6) to 54,588 sec UT (point 6') and then weakening to $0.3\mu A/m^2$ upward from 54,588 (point 6') to 54,615 sec UT (point 7) where the current density went to zero. The last two (upward) current densities are in agreement with the values obtained independently from the ESA data by direct integration of the precipitating electron flux (Table 2).
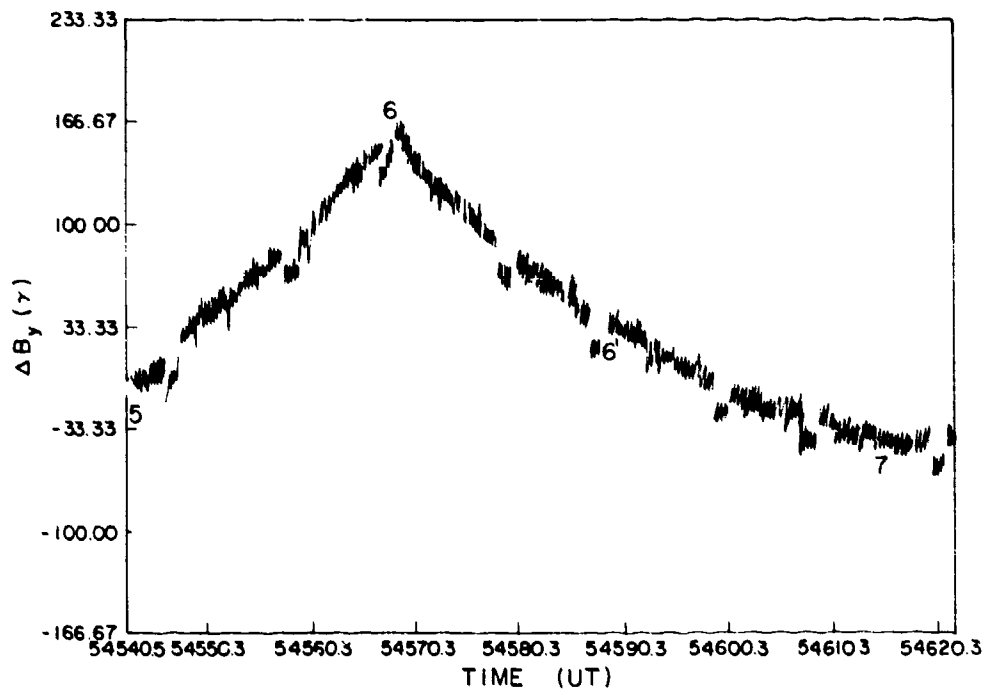

Figure 4. Variation of the Nominal East-West Component, ΔB_y, Expanded To Show the Region of the Auroral Form

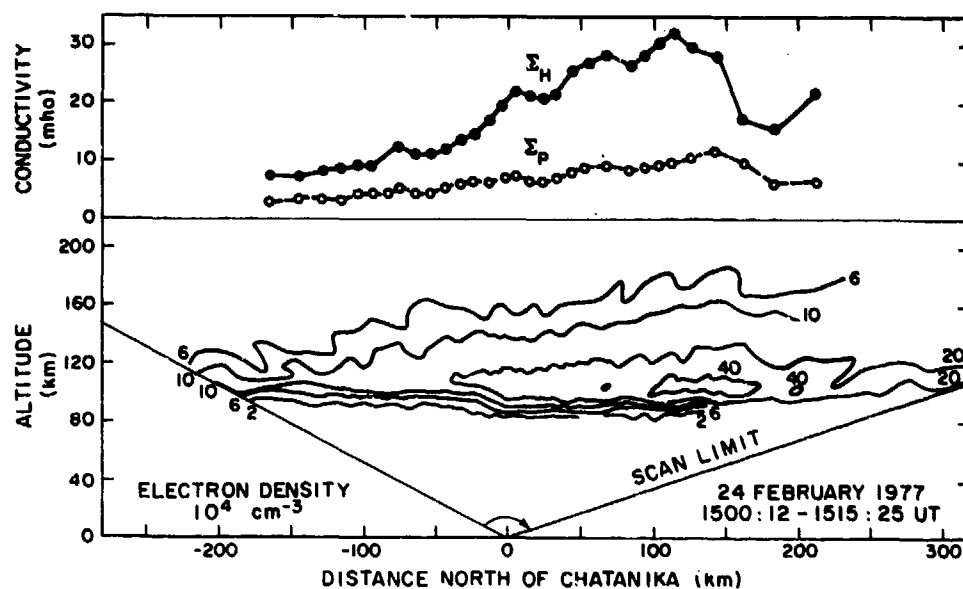Figure 5. Latitudinal Variation of Ionization and Conductivity Measured During the Elevation Scan Between 15:00:12 and 15:15:25 UT on 24 February 1977
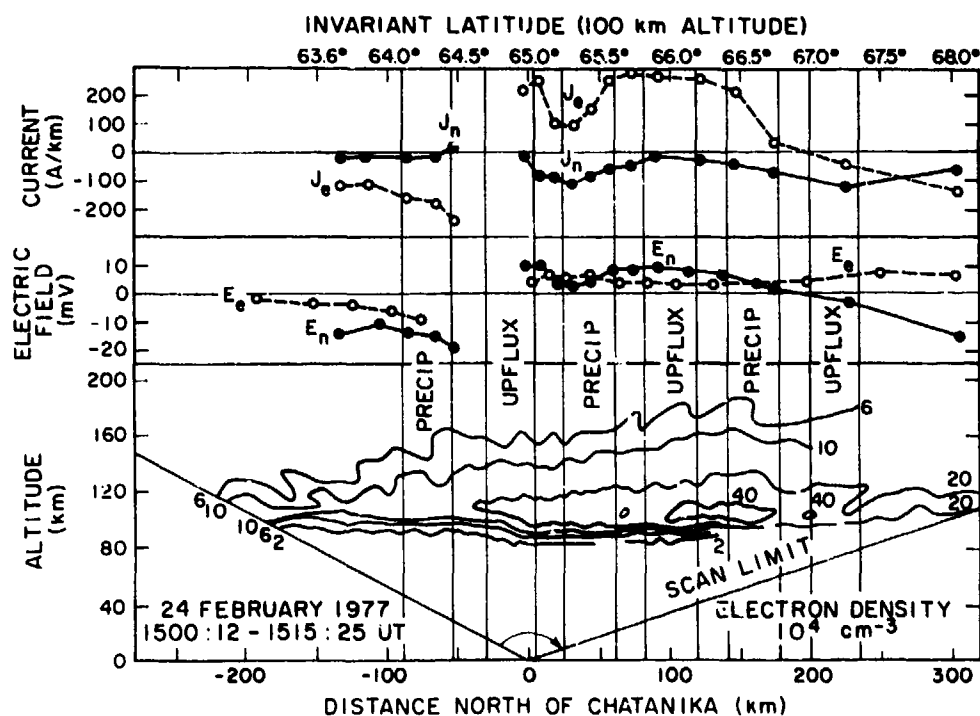
Figure 6. Latitudinal Variation of Electric Field and Electric Current Measured During the Elevation Scan Between 15:00:12 and 15:15:25 UT on 24 February 1977. Superimposed are Precipitation and Upward Flux Segments of the ESA Due to Satellite Spin.

11

The Chatanika incoherent scatter radar provides line-of-sight measurements of ion drift velocities and electron density which, using a suitable model atmosphere, can be used to determine electric fields and height-integrated Hall and Pedersen conductivities in the ionosphere. From these, the ionospheric currents may be calculated. Figures 17 and 18 (corrected) of Vondrak 1979 are reproduced here as Figures 5 and 6, respectively, showing the electron density and the derived electric field values, conductivities, and currents along the geomagnetic meridian near Chatanika during the time of passage of the S3-2 satellite.

Following the method described by Kamide and Horwitz,[4] a one-dimensional divergence of the ionospheric current, using reasonable physical approximations, may be used to calculate the field-aligned current density. Since divergence of the horizontal current flowing in the ionosphere must be balanced by field-aligned currents,

$$\text{div } J_{HORIZ} = j_{||} \tag{2}$$

where J_{HORIZ}, the height-integrated current density, is measured in A/m and $j_{||}$ in A/m^2. Since the electrojet may be assumed to be more uniform along its longer east-west dimension, Eq. (2) may be approximated as

$$j_{||} = \frac{\delta J_N}{\delta x} \tag{3}$$

where the field-aligned current density may be determined from the north-south gradient of the north current component. This may be scaled from the (corrected) current plot of Vondrak 1979, shown here as Figure 6. Since the radar data apply generally to the 100 km altitude level, and the S3-2 satellite passed overhead at an altitude of 900 km, the respectively determined current densities are plotted for comparison versus invariant latitude in Figure 7. There is a striking lack of agreement between the two field-aligned current densities with regard to direction and amplitude in the invariant latitude region of 65°-66°, just north of Chatanika. This may not be serious since horizontal drift velocities obtained directly overhead from the radar normally are considered less reliable. Further north, the agreement improves, although the upward currents differ by a factor of 2, and the boundary between up and down currents differs by 0.25° of invariant latitude. The region north of 68° is simply beyond the range of the radar measurements in the E region. The factor of 2 difference in the derived field-aligned current density values can be partially accounted for by the difference in altitude of the satellite, 900 km, and the radar data, 100 km. Considering the magnetic flux density,

---

4. Kamide, Y., and Horwitz, J. L. (1978) Chatanika radar observations of ionospheric and field-aligned currents, J. Geophys. Res. 83:1063.
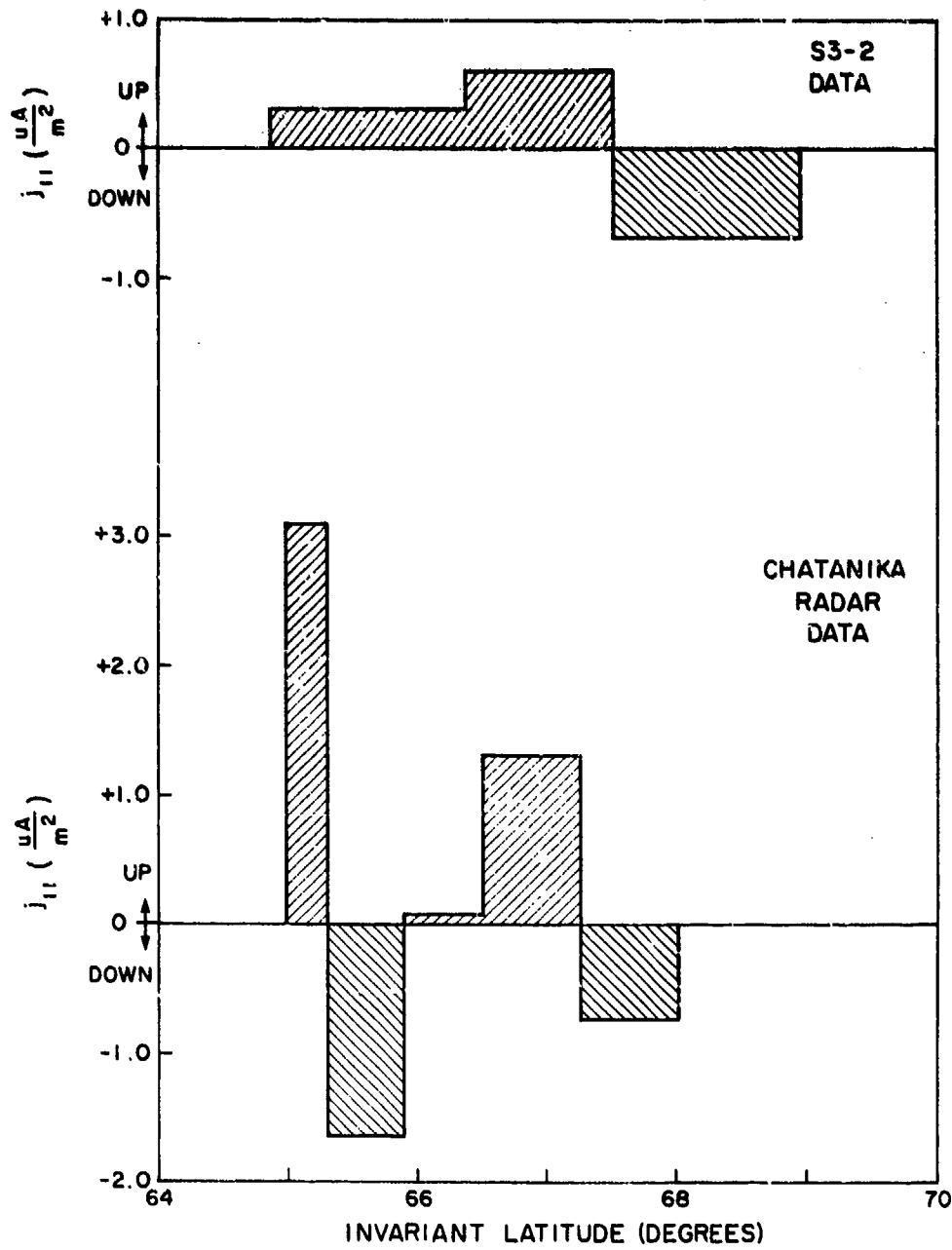
12

Figure 7. Current Densities Determined From Satellite Magnetic Data and Chatanika Radar Data

13

B, in the Faraday sense, as the number of field lines per unit cross-sectional area, and the fact that the geomagnetic field intensity increases by a factor of 1.42 when going from 900 km altitude to 100 km altitude, one would expect that as the cross-sectional area decreases, the field-aligned current density would increase by the same factor of 1.42 between the two altitude levels.

Integrating Eq. (1) and (3) piecewise with respect to x gives

$$\Delta B_y(\gamma) = \frac{\Delta J_N}{0.8} \quad (A/km) \tag{4}$$

which allows construction of a simulated satellite signature, ΔB_y, corresponding to the J_N observed by the radar. This is plotted in Figure 8 along with the spacecraft observed ΔB_y. The scale of ΔB_y in gammas indicates relative change only. As before, in Figure 7, agreement immediately north of Chatanika is very poor, but is considerably better further north.

Comparisons of the ESA data with the electron densities determined from the radar data, and the current densities determined from the fluxgate magnetometer, can be made for the region of the most intense portion of the auroral form north of Chatanika. Figure 6 shows the satellite spin segments of electrons precipitating into the ionosphere and electrons leaving the ionosphere (upflux) along the satellite trajectory expressed in invariant latitude.

Table 1 shows that the integrated electron fluxes $(cm^2 \ sec \ sr)^{-1}$ from the ESA for precipitating and upflux electrons (deduced from satellite spin) vary as the electron densities derived from the radar data, and so, also, with the intensity of the aurora. To obtain the reasonable value of J_u (up)/J_p (precipitation), the conditions in the auroral form must be somewhat similar while making the respective measurements. From Figure 6, the best conditions are for $J_p = 8.35 \times 10^8 \ (cm^2 \ sec \ sr)^{-1}$ and $J_u = 1.79 \times 10^8 \ (cm^2 \ sec \ sr)^{-1}$ where aurora is most intense. This shows the upflux to be 21.4 percent of the precipitating flux.

Table 1

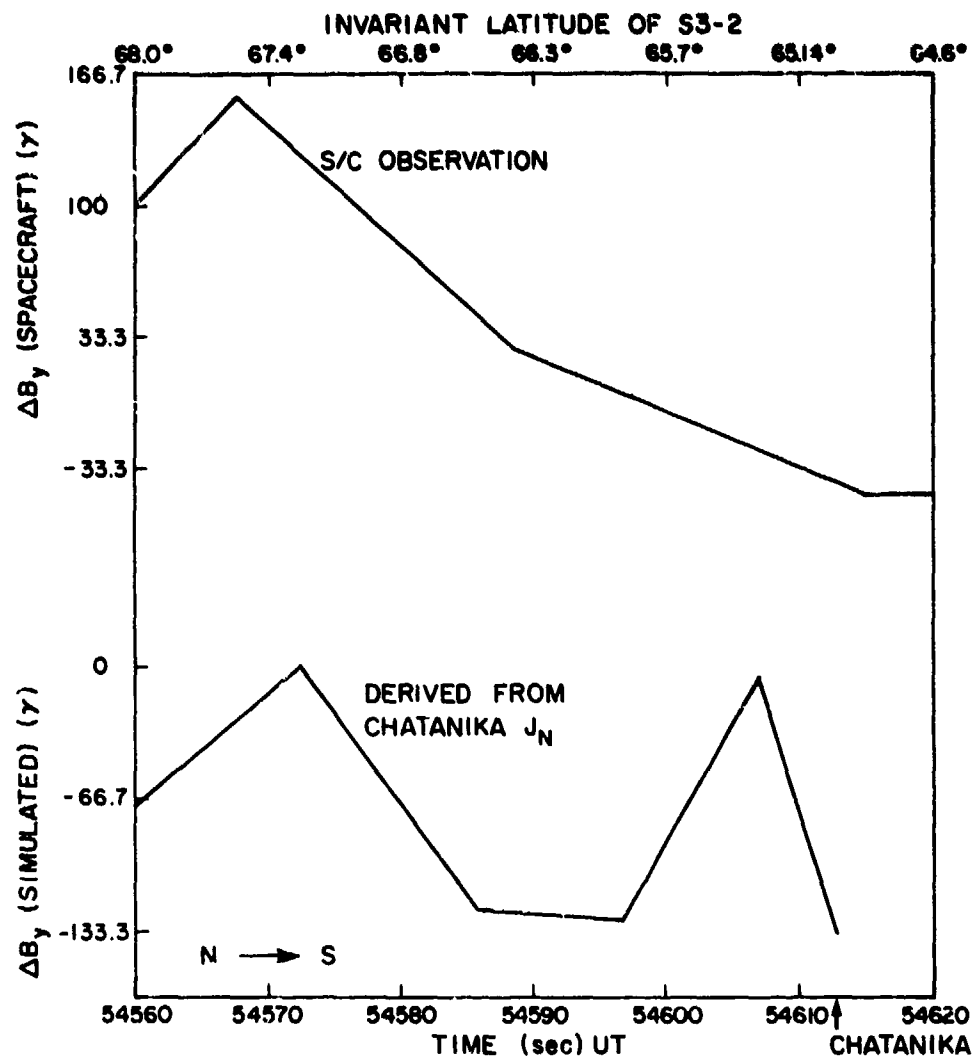| Time Period UT (sec)	Inv. Lat. (deg)	Distance from Chatanika (km)	J_T $(cm^2 sec \ sr)^{-1}$	Electron Density (cm^{-3})	J_u/J_p
54,570.73-577.29	67.35-66.98	234-199N	1.22×10^8(up)	20×10^4	> .146
54,580.95-587.39	66.78-65.41	177-141N	8.35×10^8(prec)	40×10^4	> .214
54,591.17-597.70	66.20-65.83	120- 82N	1.79×10^8(up)	$(20-40)\times10^4$	> .513
54,601.48-607.86	65.62-65.26	61- 25N	3.49×10^8(prec)	20×10^4	> .266
54,611.67-618.14	65.05-64.49	5N- 31S	9.36×10^7(up)	$(10-20)\times10^4$	

14

Figure 8. Nominal East-West Magnetic Field Component Observed by Satellite Magnetometer and the Simulated Satellite Signature, ΔB_y, Derived From the Chatanika Radar Data

Table 2 shows two periods when the ESA collected precipitating electrons, and the magnetic field data plotted in Figure 7 shows that during these periods the field-aligned currents are upward-directed. The current density was determined from the ESA data by calculating the integrated flux in spherical bands according to pitch-angle bins, and summing the results over the entire precipitation segment to obtain the total flux in $(cm^2 sec)^{-1}$, assuming azimuthal symmetry about the magnetic field line.

15

Table 2

Time Period UT (sec)	Inv. Lat (deg)	Total J $(cm^2 sec)^{-1}$	$j(\mu A/m^2)$ from ESA	from Magnetometer
54,585.10-587.39	66.6-66.4	3.30×10^8	0.53	0.6
54,601.48-604.64	65.6-65.4	2.19×10^8	0.35	0.3

As stated earlier, the current densities derived from the ESA electron data are in good agreement with those derived from the magnetometer data, both in magnitude and direction, and the integrated fluxes vary as the electron density from the radar data.

4. CONCLUDING REMARKS

The S3-2 satellite passed nearly overhead of the Chatanika radar while data were being acquired by the radar, and also by the triaxial fluxgate magnetometer and electrostatic analyzer aboard the satellite.

The current densities determined from the data of the three experiments agree quite well except in the region of invariant latitude 65°-66° which is nearly overhead and just north of the radar. Since horizontal drift velocities obtained directly overhead the radar are considered less reliable, this discrepancy may not be serious.

In the region where the auroral forms are most intense, there is excellent agreement in the variation of the precipitating electron fluxes from the ESA and the electron densities from the radar.